Derivation of fragility curves for URM school buildings in Nepal

Nicola Giordano
Research Associate, Dept. of Civil Engineering, University of Bristol, Bristol, UK

Flavia De Luca
Lecturer, Dept. of Civil Engineering, University of Bristol, Bristol, UK

Anastasios Sextos
Professor, Dept. of Civil Engineering, University of Bristol, Bristol, UK

Prem Nath Maskey
Professor, Dept. of Civil Engineering, Tribhuvan University, Kathmandu, Nepal

ABSTRACT: In recent years there has been an increasing interest from governmental authorities and Non-Governmental Organizations (NGOs) in the seismic safety enhancement of school buildings in developing countries. Schools represent a reference point for local communities and can be used as primary facilities for emergency and recovery activities after an earthquake. Focusing on the Nepal case, the last 2015 seismic events have shown that Nepalese school buildings are characterized by a high level of vulnerability. According to post-disaster surveys, more than the 20 percent of the country's classrooms experienced damage or collapse during the earthquake. Nepal's building stock is mainly constituted by non-engineered constructions realized without seismic detailing and material quality controls. Particularly, unreinforced masonry (URM) structures, representing the majority of the total building inventory, are characterized by numerous construction deficiencies such as inadequate wall-to-wall or wall-to-floor connections which have led to frequent out-of-plane collapses. Herein, a spectral-based methodology to derive fragility curves for Nepalese unreinforced masonry school buildings subjected to out-of-plane damage is discussed. The technique is applied to the case of typical mud-mortar URM Nepalese structures, by taking into account regional variations in construction practice, material properties and recurrent failure modes detected after the 2015 seismic events.

1. INTRODUCTION

In April 2015, a 7.8 magnitude earthquake followed by several aftershocks occurred in Nepal causing 8,790 deaths and almost 500,000 building collapses (Gautam and Chaulagain 2016). The seismic event significantly damaged the school facilities emphasizing the high vulnerability of these buildings. According to different post-earthquake reconnaissance reports (Aon Benfield 2015; Build Change 2015; Government of Nepal 2015; Paci-Green *et al.* 2015; EERI 2016) approximately 6,000-8,200 schools have been destroyed by the 2015 sequence of events. Post-earthquake surveys carried out adopting the inspection form from the Nepalese National Society of Earthquake Technology (NSET) resulted in 6,000 school buildings tagged with a damage grade (DG) between 4 or 5 (very heavy damage or destruction) and 11,000 tagged with DG2 or DG3 (moderate or heavy damage). The Government of Nepal has estimated the cost of damage and wider loss in the education sector to be of the order of $300-$400 million (Government of Nepal 2015; Paci-Green *et al.* 2015).

The structural configuration of most school buildings in Nepal, 89%, according to Paci-Green *et al.* (2015), consists of unreinforced masonry (URM) walls that bear both vertical and horizontal loads. In mountain areas at least 50% of them are made of rubble-stone and dry/mud mortar while in urban areas (e.g., the Kathmandu

Valley) fired-bricks with mud-mortar buildings are more recurrent (NSET 2000).

From a structural-seismic point of view, URM Nepalese school facilities are similar to residential and commercial constructions (NSET 2000). As pointed out in numerous studies, constructions in Nepal are characterized by serious structural deficiencies (Gautam and Chaulagain 2016; Gautam *et al.* 2016; Sharma *et al.* 2016; Brando *et al.* 2017). First, the floor/roof typology commonly used in URMs cannot transfer the seismic forces to the vertical bearing structure due to their high in-plane flexibility and insufficient interlocking with bearing walls that leads to insufficient diaphragm action (Gautam *et al.* 2016). Secondly, there is a lack of wall-to-wall connection between orthogonal corner walls, while seismic detailing, such as tie rods, anchors and ring beams are commonly missing. Moreover, the quality of construction is poor, leading to insufficient seismic capacity (Costa 2014). For these reasons, Nepalese masonry buildings and, among them, school buildings, are not able to respond in a monolithic box-type manner under seismic actions with the walls behaving independently and being particularly weak against out-of-plane transversal forces. This source of weakness has been more than evident in post-earthquake surveys following the 2015 event where out-of-plane failures were by far the most common damage mode observed (Build Change 2015; Government of Nepal 2015; Paci-Green *et al.* 2015; EERI 2016; Gautam and Chaulagain 2016; Gautam *et al.* 2016; Sharma *et al.* 2016; Brando *et al.* 2017).

The out-of-plane failure pattern is essentially a stability and equilibrium problem (De Felice and Giannini 2001; Doherty *et al.* 2002); thus, the lack of vertical load becomes more critical and walls with reduced axial load (i.e., non-loadbearing or at higher stories) naturally become more vulnerable (Figure 1).

Figure 1: Out-of-plane damage of Nepalese URM buildings (credits: Rama Mohan Pokhrel).

Starting from the above observations, it is evident that the out-of-plane response of walls is a key aspect for assessing the seismic vulnerability of Nepalese URM structures.

2. THE OUT-OF-PLANE VULNERABILITY ASSESSMENT OF MASONRY

As observed in numerous experimental campaigns (Shawa *et al.* 2012; Ferreira *et al.* 2015; Degli Abbati and Lagomarsino 2017), out-of-plane response of masonry walls is mostly governed by rocking. For this reason, since the first studies by Heyman (Heyman 1966a), the continuum problem has been consistently simplified by assuming the wall as a rigid body which rotates around an overturning point, triggering the so-called collapse mechanism. From a mathematical point of view, this simplification led to the development of several closed-form solutions for the calculation of the force-displacement (F-Δ) curve of a masonry wall in out-of-plane loading. With these techniques, the F-Δ diagram is usually defined as a rough bilinear (Heyman 1966), trilinear (Doherty *et al.* 2002; Lagomarsino 2015) or quadrilinear (D'Ayala and Paganoni 2011; Ferreira *et al.* 2015) backbone while laboratory tests' evidence usually shows smoother trends (Griffith *et al.* 2004; Degli Abbati and Lagomarsino 2017). Starting from these considerations, a novel analytical closed-form solution for the derivation of force-displacement curves of URM walls is herein adopted.

2.1. Mechanical-based model

The model is based on three main assumptions:

- The out-of-plane response of a vertically spanning masonry wall is purely governed by bending. This hypothesis has been largely validated in experimental tests (Griffith *et al.* 2004; Shawa *et al.* 2012; Ferreira *et al.* 2015; Degli Abbati and Lagomarsino 2017) and has been adopted in numerous mechanical-based models available in the literature (La Mendola *et al.* 1995; Godio and Beyer 2017).
- Since the nonlinear flexural deformations localize in the area with maximum bending moment (Ferreira *et al.* 2015; Degli Abbati and Lagomarsino 2017), the wall is modeled as a rigid body connected to the ground with a nonlinear hinge (Figure 2).
- The moment-rotation relationship of the nonlinear hinge is computed starting from the moment-curvature (M-χ) envelope of the critical cross-section (Figure 2). The M-χ curve is calculated under the assumption that axial strains behave linearly in bending i.e., sections remain plane. This hypothesis has been largely discussed and validated, mostly in the works of Parisi *et al.* (2016), Brencich and de Felice (2009) and Cavaleri *et al.* (2005). In this study, the closed-form M-χ relationship reported by Giordano et al. (2017) for the case of elastic-brittle no-tension masonry material is adopted. According to Crespi *et al.* (2016) the uniaxial compressive limit is assumed equal to the strength of the masonry blocks f_{mb}. The rotation θ is calculated through a constant integration of the critical cross-section's curvature over the integration length L_i.

The model is capable to represent three boundary configurations i.e., cantilever, pinned-pinned and clamped-clamped wall by introducing the quantity h_{LV}, i.e., the shear length of the wall. The integration length L_i, calibrated through analytical-experimental comparisons, is assumed equal to $0.25 \cdot h_{LV}$.

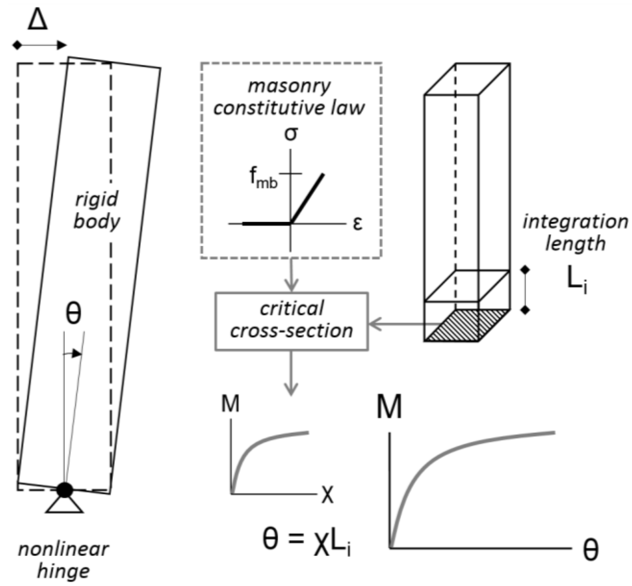

Figure 2: Mechanical-based model for the out-of-plane assessment of URM walls.

2.2. Vulnerability assessment procedure

Considering the deficiencies of typical Nepali URM buildings, the vulnerability assessment methodology here adopted is based on three main assumptions: (i) the only considered failure mode is the out-of-plane, (ii) the walls of the structure behave independently, (iii) the vulnerability of the whole building is ruled by the wall with the worst seismic performance calculated through well consolidated spectral-based techniques. In details, the vulnerability procedure consists in a three steps analysis:

1. *Walls classification*. The walls of the building are classified with respect to their boundary conditions and overburden axial load.
2. *Force-displacement curve calculation and Damage States (DS) definition.* The F-Δ curves of any wall configuration are calculated with the closed-form solution described in 2.1. Subsequently damage thresholds are directly estimated on the F-Δ diagram according to well consolidated procedures available in the literature (Rota *et al.* 2010; Lagomarsino 2015).
3. *Intensity Measure (IM) estimation for corresponding DS.* IMs correspondent to any DSs are estimated with the Capacity Spectrum

Method (CSM) (Freeman 2004). Particularly, the modified version of the CSM developed by Lagomarsino (2015) for the out-of-plane vulnerability assessment of masonry structures is herein utilized. The procedure is based on the following steps: (i) the *F-Δ* curve is transformed into a capacity curve defined in a pseudo-acceleration (S_a) versus pseudo-displacement (S_d) plane; (ii) from the DS defined on the capacity curve, the corresponding periods T_{DS} and equivalent damping coefficients ξ_{DS} are evaluated (Lagomarsino and Cattari 2015); (iii) calculation of Acceleration Displacement Response Spectrum (ADRS) and estimation of the IM by scaling the ADRS shape in order to intersect the capacity curve at the given DS (Lagomarsino 2015). Since the Nepalese Building Code (DUDBC 1994) does not provide elastic response spectrum equations, the Type I spectral shape of the Eurocode 8 (EC8 2004) is used. It is worth noting that for the walls located at the upper floors specific amplified response spectra have to be considered (Suarez and Singh 1987). In the present study the floor spectral equations proposed by Lagomarsino (2015) are adopted.

3. INPUT VARIABLES

The procedure described before can be used for the derivation of fragility curves of Nepalese URM buildings by performing a Monte Carlo simulation where the variability of the input parameters of the model are directly taken into account. Among the four recurrent URM typologies present in Nepal (i.e., stone-mud, stone-cement, brick-mud and brick-cement (ARUP 2015)), this work focuses on URM brick mud-mortar buildings since they are widespread among the country and, at least in the Kathmandu Valley, they represent 45% of the URMs (NSET 2000). The main characteristics of these buildings are: 1-to-4 stories elevation; inter-story height of 2.7 m; bearing wall thickness between 35 cm and 45 cm; presence of traditional flexible floors (earth laid on wooden planks, supported by timber or bamboo joists); presence of light corrugated galvanized iron (CGI) roofs supported by timber joists; absence of seismic detailing, ring beams or anchors; inadequate wall-to-wall connections (ARUP 2015).

As discussed in Section 2, the vulnerability assessment procedure consists in determining the IM_{DS} for any wall configuration and selecting the minimum value as representative of the entire building. Given the damage evidence observed during several post Gorkha earthquake surveys, (EERI 2016; Sharma *et al.* 2016; Brando *et al.*, 2017), the present study considers the wall configurations reported in Figure 3: (i) full-height non-loadbearing walls with cantilever boundary condition, (ii) upper stories non-loadbearing walls in cantilever configuration, (iii) lower stories loadbearing walls with clamped-clamped boundaries, (iv) top-story loadbearing walls in cantilever configuration. Subsequently, the input variables of the assessment procedure are defined as a set of probabilistic distributions, more specifically: number of stories, story height, walls thickness, masonry's elastic modulus (E_m), bricks compressive strength (f_{mb}), masonry specific weight (γ_m), roof and floor weight and corresponding structural midspan.

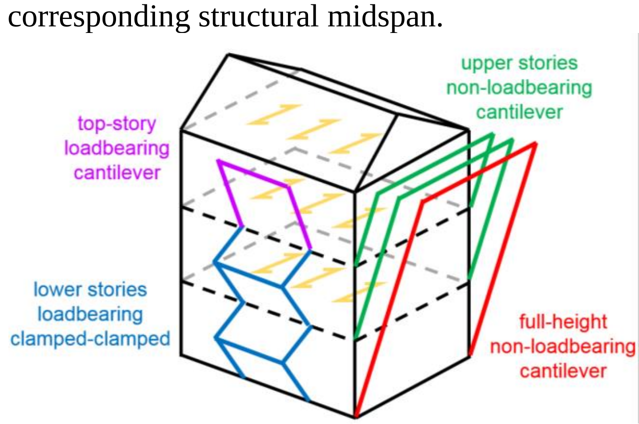

Figure 3: Walls configurations considered in the vulnerability analysis.

Table 1 reports the type and parameters of these probabilistic distributions while percentage distributions of the number of floors and Probability Density Functions (PDFs) for E_m and f_{mb} are shown in Figures 4 to 6, respectively. Additional variability has been included in the CSM method by considering uniform distributions for the initial damping ξ_0 (ranging from 3% to 5%) and for the equivalent asymptotic hysteretic damping (ranging from 5% to 20%) as for Lagomarsino and Cattari (2015).

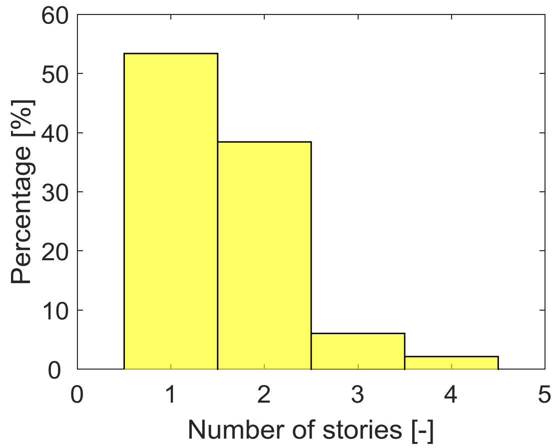

Figure 4: Number of stories distribution.

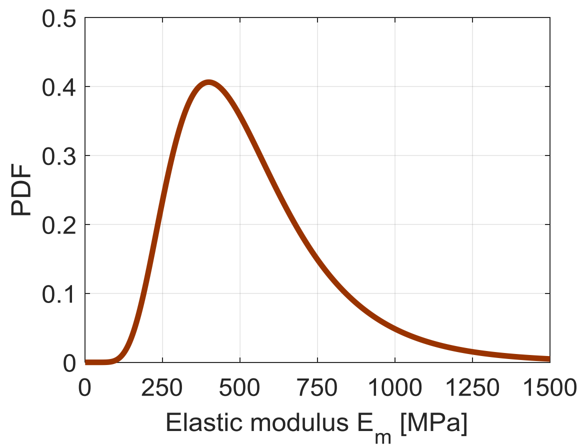

Figure 5: Probability density function for the masonry elastic modulus E_m.

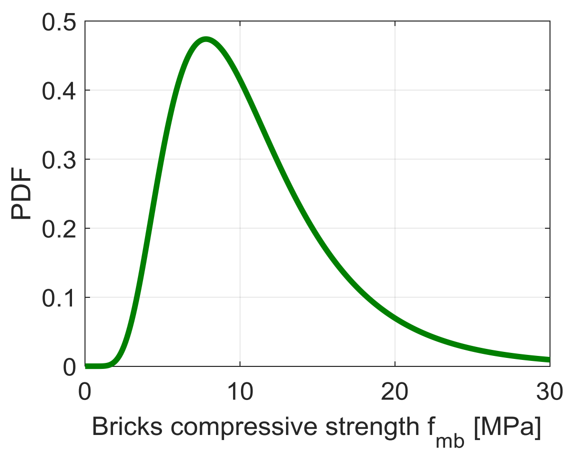

Figure 6: Probability density function for the bricks compressive strength f_{mb}.

Table 1: Parameter values adopted in the analysis and assumed probabilistic distributions.

Number of stories: piecewise uniform distribution *Ref.: (NSET 2000)*				
[-]	1	2	3	4
[%]	53.38	38.43	6.05	2.14
Story height: normal truncated distribution *Ref.: (ARUP 2015)*				
μ [m]	2.7			
CoV [-]	0.3			
lim [m]	2.4	3.0		
Wall thickness: uniform distribution *Ref.: (ARUP, 2015)*				
min [cm]	35			
max [cm]	45			
Section thickness reduction factor: uniform distribution *Ref.: (Lagomarsino, 2015)*				
min [-]	0.7			
max [-]	1.0			
Masonry elastic modulus: lognormal distribution *Ref.: (Rits-DMUCH 2012)*				
μ [MPa]	537.25			
CoV [-]	0.469			
Bricks compressive strength: lognormal distribution *Ref.: (Sarangapani et al. 2005; Rits-DMUCH 2012)*				
μ [MPa]	11.03			
CoV [-]	0.51			
Masonry specific weight: lognormal distribution *Ref.: (Graubner and Brehm 2011; Rits-DMUCH 2012)*				
μ [kN/m^3]	17.68			
CoV [-]	0.05			
Floor load: lognormal distribution *Ref.: (BIS 1987)*				
μ [kN/m^2]	3.10			
CoV [-]	0.10			
CGI roof load: lognormal distribution *Ref.: (BIS 1987)*				
μ [kN/m^2]	0.15			
CoV [-]	0.22			
Midspan: normal truncated distribution *Ref.: (NSET 2000)*				
μ [m]	1.5			
CoV [-]	0.3			
lim [m]	1.0	2.0		
μ: average value; CoV: coefficient of variation				

4. RESULTS

Monte Carlo simulation has been performed by randomly generating N = 100,000 combinations of the input parameters reported in Table 1. The number N of realizations has been estimated by calculating the mean and standard deviation of the output for increasing N until a three digits precision of the output was reached. In order to evaluate the effect of the number of stories on the final fragility results, the Monte Carlo has been repeated for: (a) one-story buildings only; (b) 2-to-4 multistory buildings; (c) story distribution according to Table 1. Figure 7 reports the results of the analysis in terms of fragility functions while in Table 2 are indicated median values η and dispersions β for the different DS. Among the various probability models suitable for fragility curves definition (De Risi *et al.* 2017), lognormal distribution has been considered in this study.

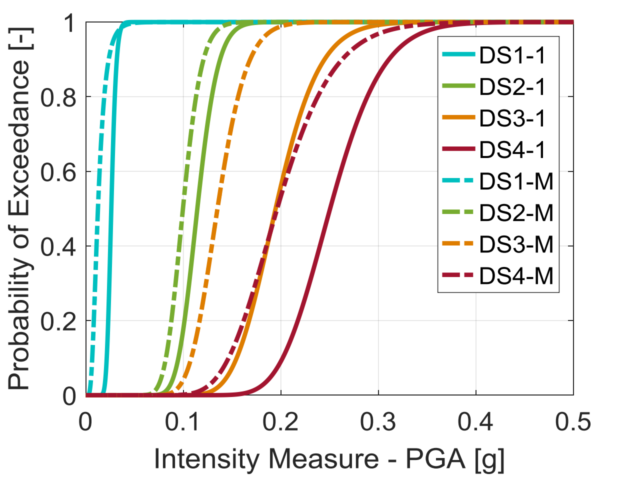

Figure 7: Damage Fragilities for 1-story and Multi-story buildings.

Table 2: Median values and dispersion for 1-story and Multi-story buildings.

	DS1		DS2		DS3		DS4	
	η	β	η	β	η	β	η	β
1	0.026	0.15	0.11	0.14	0.19	0.18	0.25	0.17
M	0.012	0.49	0.10	0.15	0.13	0.17	0.20	0.22

As expected, the median IM values for the multi-story case are lower than the ones related to single story buildings while the dispersion results are larger (Table 2). This outcome could be easily justified since the top floor walls in multi-story buildings are affected by a more severe ADRS. The more severe floor ADRS leads to more restrictive IM values which, in turn, lower the 50th percentile and increase the scattering.

Figure 8 reports the histograms related to the Monte Carlo simulations for the URM building stock as per piecewise distribution in Table 1. Lastly, the results of the simulations are compared with observational damage fragilities available in the literature, derived for the Nepalese building stock (Chaulagain *et al.* 2016; Gautam et al. 2018). Table 3 reports corresponding median and dispersion values.

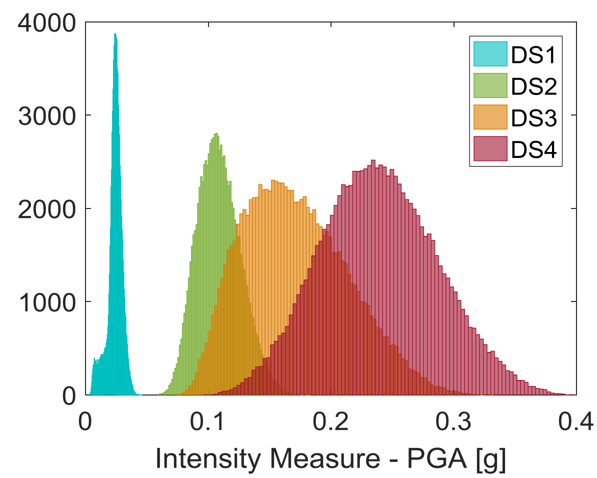

Figure 8: PGA histograms for the Monte Carlo simulation.

Table 3: Median values and dispersion for URM according to this study (S), Chaulagain et al. 2016 (C) and Gautam et al. 2018 (G).

	DS1(S)		DS2(S) Moderate(C) DS-1(G)		DS3(S) Extensive(C) DS-2(G)		DS4(S) Collapse(C) DS-3(G)	
	η	β	η	β	η	β	η	β
S	0.025	0.24	0.11	0.16	0.17	0.24	0.24	0.20
C	-	-	0.12	0.72	0.19	0.72	0.35	0.66
G	-	-	0.13	0.38	0.16	0.42	0.22	0.48

5. CONCLUSIONS

A spectral-based approach based on the out-of-plane assessment of masonry walls has been employed to derive fragility curves for the URM Nepalese school building stock. Subsequently a Monte Carlo simulation has been proposed to obtain analytical fragilities of URM school buildings made of clay bricks and mud-mortar.

The distribution of the input variables used in the Monte Carlo is tailored to the characteristics of the Nepali school buildings portfolio. The study has shown that analytical fragilities 50th percentiles are in good agreement with the ones from observational fragilities of Nepalese URMs available in the literature. On the contrary, the dispersions estimated analytically remain consistently lower than the observational values. However, this limitation could be overcome by considering the record-to-record variability (De Luca *et al.* 2014, Rossetto *et al.* 2016) i.e. substituting the EC8 spectral shape with a set of recorded ground motions ADRS shapes. This aspect, that was not investigated in this preliminary study, will be addressed in future publications.

ACKNOWLEDGEMENTS

This work was funded by the Engineering and Physical Science Research Council (EPSRC) under the project "Seismic Safety and Resilience of Schools in Nepal" SAFER (EP/P028926/1).

REFERENCES

Aon Benfield (2015) *2015 Nepal Earthquake Event Recap Report*. London, UK.

ARUP (2015) *Global Program for Safer Schools - Structural Typologies*. London, UK.

Brando, G. *et al.* (2017) 'Damage Reconnaissance of Unreinforced Masonry Bearing Wall Buildings After the 2015 Gorkha, Nepal, Earthquake'. *Earthquake Spectra*, 33, pp. 243–273.

Brencich, A. and de Felice, G. (2009) 'Brickwork under eccentric compression: Experimental results and macroscopic models', *Construction and Building Materials*, 23(5), pp. 1935–1946.

Build Change (2015) *April 25, 2015 – Gorkha Earthquake, Nepal*. Denver, USA.

Bureau of Indian Standards (BIS) (1987) *IS 875: Code of Practice for Design Loads (Other Than Earthquake) For Buildings and Structures*. New Delhi, India.

Cavaleri, L. *et al.* (2005) 'Experimental and analytical response of masonry elements under eccentric vertical loads', *Engineering Structures*, 27(8), pp. 1175–1184.

Chaulagain, H. *et al.* (2016) 'Earthquake loss estimation for the Kathmandu Valley', *Bulletin of Earthquake Engineering*, 14(1), pp. 59–88.

Costa, A. (2014) *Structural Rehabilitation of Old Buildings*. Springer Netherlands.

Crespi, P. *et al.* (2016) 'Structural analysis of stone masonry columns of the Basilica S. Maria di Collemaggio', *Engineering Structures*, 129, pp. 81–90.

D'Ayala, D. F. and Paganoni, S. (2011) 'Assessment and analysis of damage in L'Aquila historic city centre after 6th April 2009', *Bulletin of Earthquake Engineering*, 9(1), pp. 81–104.

Degli Abbati, S. and Lagomarsino, S. (2017) 'Out-of-plane static and dynamic response of masonry panels', *Engineering Structures*, 150, pp. 803–820.

De Luca, F. *et al*. (2014) 'The structural role played by masonry infills on RC building performances after the 2011 Lorca, Spain, earthquake', *Bulletin of Earthquake Engineering*, 12, pp. 1999–2026.

DUDBC Department of Urban Development and Building Construction. (1994). *Nepal National Building Code*. Kathmandu, Nepal.

Doherty, K. *et al.* (2002) 'Displacement-based seismic analysis for out-of-plane bending of unreinforced masonry walls', *Earthquake Engineering and Structural Dynamics*, 31(4), pp. 833–850.

EC8 Design of structures for earthquake resistance - Part 1 : General rules, seismic actions and rules for buildings (2004), Brussels, Belgium.

EERI Earthquake Engineering Research Institute (2016) *M7.8 Gorkha, Nepal Earthquake on April 25, 2015 and its Aftershocks*. Oakland, CA, USA.

de Felice, G. and Giannini, R. (2001) 'Out-of-plane seismic resistance of masonry walls', *Journal of Earthquake Engineering*, 5(2), pp. 253–271.

De Risi *et al.* (2017) 'Bayesian tsunami fragility modeling considering input data uncertainty', *Stochastic Environmental Research and Risk Assessment* 31, pp. 1253–1269.

Ferreira, T. M. *et al.* (2015) 'A simplified four-branch model for the analytical study of the out-of-plane performance of regular stone URM walls', *Engineering Structures*, 83, pp. 140–153.

Ferreira, T. M. *et al.* (2015) 'Experimental characterization of the out-of-plane performance of regular stone masonry walls, including test setups and axial load influence', *Bulletin of Earthquake Engineering*, 13(9), pp. 2667–2692.

Freeman, S. A. (2004) 'Review of the development of the capacity spectrum method', *ISET Journal of Earthquake Technology*, 41(1), p. 113.

Gautam, D. *et al.* (2016) 'Common structural and construction deficiencies of Nepalese buildings', *Innovative Infrastructure Solutions*, 1(1), p. 1.

Gautam, D. and Chaulagain, H. (2016) 'Structural performance and associated lessons to be learned from world earthquakes in Nepal after 25 April 2015 (MW 7.8) Gorkha earthquake', *Engineering Failure Analysis*, 68, pp. 222–243.

Gautam, D., Fabbrocino, G. and Santucci de Magistris, F. (2018) 'Derive empirical fragility functions for Nepali residential buildings', *Engineering Structures*, 171, pp. 617–628.

Giordano, N., Crespi, P. and Franchi, A. (2017) 'Flexural strength-ductility assessment of unreinforced masonry cross-sections: analytical expressions', *Engineering Structures*, 148, pp. 399–409.

Godio, M. and Beyer, K. (2017) 'Analytical model for the out-of-plane response of vertically spanning unreinforced masonry walls', *Earthquake Engineering and Structural Dynamics*, 46(15), pp. 2757–2776.

Government of Nepal (2015) *Nepal Earthquake 2015 - Post Disaster Needs Assessment*. Kathmandu, Nepal.

Graubner, A. and Brehm, E. (2011) *JCSS Probabilistic Model Code - Part 3: Resistance Models - 3.2 Masonry Properties*.

Griffith, M. C. *et al.* (2004) 'Experimental Investigation of Unreinforced Brick Masonry Walls in Flexure', *Journal of Structural Engineering*, 130(3), pp. 423–432.

Heyman, J. (1966) 'The stone skeleton', *International Journal of Solids and Structures*, 2(2), pp. 249–279.

Lagomarsino, S. (2015) 'Seismic assessment of rocking masonry structures', *Bulletin of Earthquake Engineering*, 13(1), pp. 97–128.

Lagomarsino, S. and Cattari, S. (2015) 'PERPETUATE guidelines for seismic performance-based assessment of cultural heritage masonry structures', *Bulletin of Earthquake Engineering*, 13(1), pp. 13–47.

La Mendola, L., Papia, M. and Zingone, G. (1995) 'Stability of Masonry Walls Subjected to Seismic Transverse Forces', *Journal of Structural Engineering*, 121(11), pp. 1581–1587.

National Society for Earthquake Technology (NSET) (2000) *Seismic vulnerability of the public school buildings of Kathmandu Valley and methods for reducing it*. Kathmandu, Nepal.

Paci-Green, R., Pandley, B. and Friedman, R. (2015) *Post-earthquake comparative assessment of school reconstruction and social impacts in Nepal*. USA.

Parisi, F., Sabella, G. and Augenti, N. (2016) 'Constitutive model selection for unreinforced masonry cross sections based on best-fit analytical moment-curvature diagrams', *Engineering Structures*, 111, pp. 451–466.

Rits-DMUCH (Research Center for Disaster Mitigation of Urban Cultural Heritage) (2012) *Disaster Risk Management for the Historic City of Patan, Nepal*. Kyoto, Japan.

Rossetto, T., Gehl, P., Minas, S., Galasso, C., Duffour, P., Douglas, J., and Cook, O. (2016) 'FRACAS: A capacity spectrum approach for seismic fragility assessment including record-to-record variability', *Engineering Structures*, 125, pp. 337–348.

Rota, M., Penna, A. and Magenes, G. (2010) 'A methodology for deriving analytical fragility curves for masonry buildings based on stochastic nonlinear analyses', *Engineering Structures*, 32(5), pp. 1312–1323.

Sarangapani, G., Venkatarama, B. V. and Jagadish, K. S. (2005) 'Brick-Mortar Bond and Masonry Compressive Strength', *Journal of Materials in Civil Engineering*, 17, pp. 229–237.

Sharma, K., Deng, L. and Noguez, C. C. (2016) 'Field investigation on the performance of building structures during the April 25, 2015, Gorkha earthquake in Nepal', *Engineering Structures*, 121, pp. 61–74.

Shawa, O. Al *et al.* (2012) 'Out-of-plane seismic behaviour of rocking masonry walls', *Earthquake Engineering and Structural Dynamics*, 41(5), pp. 949–968.

Suarez, L. E. and Singh, M. P. (1987) 'Floor response spectra with structure-equipment interaction effects by a mode synthesis approach', *Earthquake Engineering & Structural Dynamics*, 15, pp. 141–158.